Josephson-coupled systems in perpendicular magnetic fields

L. L. Daemen, L. N. Bulaevskii, M. P. Maley, and J. Y. Coulter
Theoretical Division and Superconductivity Technology Center, Los Alamos National Laboratory, Los Alamos, New Mexico 87545
(Received 9 November 1992)

We calculate the critical current along the c axis of a stack of Josephson-coupled layers when the applied magnetic field is perpendicular to the junctions plane. The anisotropy parameter and the Josephson interlayer critical current in the Lawrence-Doniach model are renormalized by the vortex fluctuations and have to be determined self-consistently. This leads to the existence of a decoupling phase transition in the (H,T) plane. The decoupling phase transition is first order for moderate (bare) anisotropies and second order for large anisotropies. We consider the effect of pinning centers and show that only strong disorder affects the critical current. Application of the formalism to single crystals, tapes, and films of highly anisotropic, layered superconductors is discussed. The magnetic field and temperature dependence of the critical current in tapes is calculated for the brick-wall model.

I. INTRODUCTION

The distinguishing feature of the high-T_c superconductors is the existence of superconducting, Josephson-coupled layers. The consequences of this peculiar structure are manifold and to a large extent responsible for the unusual electrodynamic properties of these materials in the superconducting state. These systems seem to be well described by the Lawrence-Doniach (LD) formalism,[1] which is often used as a conceptual framework to interpret experimental data. We point out that the most important parameter of the model, the anisotropy parameter $\gamma = \lambda_c/\lambda_{ab}$, depends strongly on the temperature in the presence of magnetic field perpendicular to the layers. It has to be calculated self-consistently when a magnetic field is applied perpendicular to the layers. For this reason, the anisotropy parameter acquires a field and temperature dependence it does not have in the more conventional Ginzburg-Landau (GL) model. The c-axis critical current is inversely proportional to γ^2 and is a physical quantity directly accessible to experiment. It displays most dramatically and directly the consequences of the renormalization of γ. Therefore, the present article focuses on the critical current along the c axis in these systems in the presence of a magnetic field applied perpendicular to the layers.

More pragmatically, the "Lorenz-force-free" configuration considered here is important for two other reasons. First, recent magnetoresistivity measurements by Kapitulnik[2] and Briceño, Crommie, and Zettl[3] of the resistivity in the c direction (with the applied magnetic field parallel to the c axis) show a remarkable behavior below T_c that was interpreted in terms of a decoupling transition. We show that the existence of this phase transition is directly related to the peculiar form of the LD free-energy functional and is a new and distinctive feature of Jospehson-coupled systems as opposed to the GL description.

Second, it is well-known experimentally that the critical current of films and tapes of the high-T_c materials is lower when the external field is applied perpendicular to the layers than when the field is applied parallel to the layers.[4,5] In order to account for the dependence of the critical current on magnetic field and temperature, the brick-wall model was suggested[6,7] as a crude way to take into account the material microstructure. In this model, the current flows mostly inside the grains ("bricks") making up the tape (or film) but is forced to transfer along a c-axis grain boundary to flow from one grain to the next. The critical current associated with that weak link is lower than the bulk critical current inside a grain and constitutes the bottleneck for current transport along a tape. The effect on the Josephson intergrain current of a magnetic field parallel to the layers was calculated in Ref. 7, but the effect of a perpendicular field was not considered.

Below we discuss in detail the physical mechanism responsible for the reduction of the critical current in perpendicular fields and calculate the temperature dependence of the decoupling field. We also determine the nature of the phase transition that takes place at the decoupling field. We believe the mechanism responsible for the depression of the critical current density in perpendicular fields to be the following. The magnetic field nucleates pancake vortices in the layers.[8,9] These two-dimensional vortices are coupled electromagnetically as well as by the presence of Jospehson tunneling between the layers. If the vortices are perfectly aligned from one layer to the next, their coupling is maximal and so is the critical current density. However, if a pancake vortex is displaced from its equilibrium position (thermal distortion or pinning for example) a phase difference is generated across two adjacent layers and the critical current is reduced locally [Fig. 1(a)]. (Because of the *nonlinear*, *sinusoidal* dependence of the interlayer current on the phase difference, the appearance for whatever reason of a finite phase difference *reduces* the current density.) It is this reduction of the local value of the Josephson current due to the misalignement of the pancake vortices that is responsible for the lower value of the critical current density when

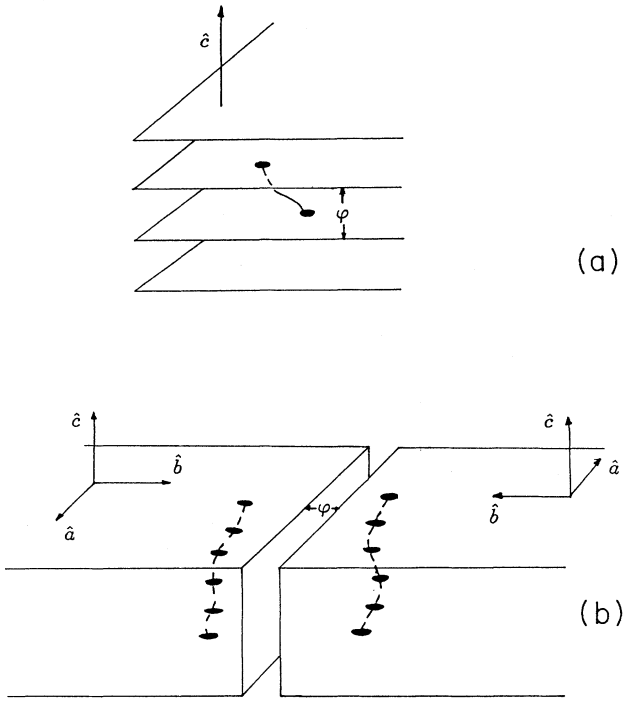

FIG. 1. Schematic representation of the two types of Josephson-coupled systems considered in the text. (a) Stack of Josephson-coupled superconducting layers and (b) Josephson junction parallel to the c axis.

the magnetic field is applied perpendicular to the layers. In addition, the square of the London penetration depth in the $\hat{c}$ direction, λ_c, is inversely proportional to the critical current density j_c, which in turn depends on the disorder in the vortex positions. The lattice distortions are determined by the elastic moduli, which depend on λ_c, and therefore λ_c and j_c have to be determined self-consistently. It is this self-consistence, absent in the GL formalism, that is responsible for the existence of the decoupling phase transition. Notice that in the GL formalism, the relationship between the current density and the phase difference is *linear* insofar as the the magnitude of the order parameter remains constant (London limit). A similar mechanism of the supression of critical current by the vortex fluctuations is at work in a Josephson junction when the external field is applied parallel to the junction plane and pancake vortices are nucleated in the superconductors making up the junction [Fig. 1(b)]. This situation is discussed briefly below. A more detailed account within the framework of Malozemoff's brick-wall model will be given elsewhere.

The local supression of the current density by two misaligned Abrikosov vortices in a Josephson junction was studied originally by Miller *et al.*[10] Recently, Glazman and Koshelev pointed out that the thermal fluctuations of pancake vortices supress the superconducting long-range order along the c axis,[11] but they did not study the behavior of the critical current and did not take into account in a self-consistent manner the renormalization of the current and anisotropy parameter. A summary of some of the results presented here appeared in Ref. 12.

The next section describes in more detail the physical mechanism sketched above and develops the LD formalism when the external field is perpendicular to the layers. Sections III and IV deal with various sources of disorder, namely thermal distortions of the lattice and pinning-induced disorder. These two types of disorder are quite distinct, and they affect the critical current in totally different ways. In addition, Section III discusses the c-axis resistivity. Section V applies the results obtained in Secs. III and IV to the particular case of films and tapes within the framework of the brick-wall model. We state our conclusions in the last section.

II. MODEL AND FORMALISM

The LD model for the highly anisotropic layered superconductors is well established by now and has been used extensively and successfully to describe the properties of the high-temperature superconductors at the phenomenological level. The essence of the formalism is the Josephson nature of the interlayer coupling, and, correspondingly, of the interlayer current. In the LD formalism, the current density, $j_{n,n+1}$, between layers n and $n+1$ is defined by

$$j_{z;n,n+1}(\boldsymbol{\rho}) = j_0 \sin[\varphi_{n,n+1}(\boldsymbol{\rho})], \tag{2.1}$$

$$\varphi_{n,n+1}(\boldsymbol{\rho}) = \phi_n - \phi_{n+1} - \frac{2\pi}{\Phi_0}\int_{ns}^{(n+1)s} A_z(\mathbf{r})dz, \tag{2.2}$$

where $\varphi_{n,n+1}(\boldsymbol{\rho})$ is the gauge-invariant phase difference. $\phi_n(\boldsymbol{\rho})$ is the phase of the order parameter in the nth layer, s is the interlayer spacing, and $A_z(\mathbf{r})$ is the c-axis component of the vector potential. $\boldsymbol{\rho} = (x, y)$ designates coordinates in the ab plane and $\mathbf{r} = (\boldsymbol{\rho}, z)$. j_0 depends on the value of the order parameter inside the layers as well as on temperature and magnetic field, just as for standard Josephson junctions.[13] The critical current j_0 along the c axis determines the London penetration depth for that direction (and consequently the anisotropy parameter):

$$\lambda_c^2 = \frac{c\Phi_0}{8\pi^2 s j_0}, \quad \gamma = \frac{\lambda_c}{\lambda_{ab}}. \tag{2.3}$$

The form of the LD free-energy functional considered here is

$$\mathcal{F}\{\phi_n(\mathbf{r}), \mathbf{A}(\mathbf{r})\} = \frac{\Phi_0^2 s}{32\pi^3\lambda_{ab}^2}\sum_n \int d\mathbf{r}\left[\left(\nabla\phi_n + \frac{2\pi}{\Phi_0}\mathbf{A}_n\right)^2 + \frac{2}{\lambda_J^2}(1-\cos\varphi_{n,n+1})\right] + \int d\mathbf{r}\,\frac{h^2}{8\pi}, \tag{2.4}$$

where $\lambda_J \equiv \gamma s$ is the Josephson length and λ_{ab} is the London penetration depth in the ab plane. The amplitude of the superconducting order parameter has been assumed constant. This approximation is correct to the extent that

we are interested only in considering the effect of the Josephson coupling between the layers. Notice that in what follows, we neglect the effect of the the normal cores on the interlayer tunneling current because of their small size in high-T_c materials.

In order to obtain a general expression for the critical current density in the presence of pancake vortices, we use the following equation relating the gauge-invariant phase difference $\varphi_{n,n+1}(\boldsymbol{\rho})$ to the positions of the vortices:[14]

$$\boldsymbol{\nabla}^2\varphi_{n,n+1} - \frac{1}{\lambda_J^2}(2\sin\varphi_{n,n+1} - \sin\varphi_{n+1,n+2} - \sin\varphi_{n-1,n}) - \frac{1}{\lambda_c^2}\sin\varphi_{n,n+1} = 0, \tag{2.5}$$

which should be solved with the boundary condition:[15]

$$(\nabla_x\nabla_y - \nabla_y\nabla_x)\varphi_{n,n+1} = \sum_{\mathbf{m}} 2\pi[\delta(\boldsymbol{\rho} - \boldsymbol{\rho}_{n\mathbf{m}}) - \delta(\boldsymbol{\rho} - \boldsymbol{\rho}_{n+1;\mathbf{m}})], \tag{2.6}$$

where $\boldsymbol{\rho}_{n\mathbf{m}} = (x_{n\mathbf{m}}, y_{n\mathbf{m}})$ are the positions of the two-dimensinal (2D) vortices in the nth layer. The second index $\mathbf{m}$ labels the pancakes in a given layer. The Dirac δ functions in the right-hand side of Eq. (2.6) indicate the presence of vortices. Notice that the right-hand side of Eq. (2.6) vanishes for straight, undistorted vortices for which $\boldsymbol{\rho}_{n\mathbf{m}} = \boldsymbol{\rho}_{n+1;\mathbf{m}}$. In this case $\varphi_{n,n+1}(\boldsymbol{\rho}) = 0$. It follows from Eq. (2.5) that at distances smaller than λ_J away from the vortices, the effect of the interlayer Josephson current is negligible and the main contribution to the phase difference at $\boldsymbol{\rho}$ can then be obtained by solving a linearized form of Eq. (2.5), namely the following 2D Laplace equation with the boundary condition, Eq. (2.6):

$$\boldsymbol{\nabla}_\rho^2\,\varphi_{n,n+1}(\boldsymbol{\rho}) = 0: \tag{2.7}$$

The general solution of this equation is given by

$$\varphi_{n,n+1}(\boldsymbol{\rho}) = \sum_{\mathbf{m}}\left(\arctan\frac{x - x_{n\mathbf{m}}}{y - y_{n\mathbf{m}}} - \arctan\frac{x - x_{n+1;\mathbf{m}}}{y - y_{n+1;\mathbf{m}}}\right). \tag{2.8}$$

The physical origin of Eq. (2.8) is easy to understand. In layer n, a vortex located at $\boldsymbol{\rho}_{n\mathbf{m}}$ contributes a phase $\phi_n(\boldsymbol{\rho})$ at $\boldsymbol{\rho}$. This angle ϕ_n is simply the polar angle around $\boldsymbol{\rho}_{n\mathbf{m}}$. Notice that this result differs from that given in Refs. 16–18 where other definitions of the phase difference were introduced [the definitions given by these authors are not solutions of Eq. (2.5) or its linearized form]. In order to take into account the 3D screening caused by the interlayer currents, we approximate $\sin\varphi_{n,n+1}$ by $\varphi_{n,n+1}$ and express the latter in terms of the distortions $u_{n\mathbf{m}} = \boldsymbol{\rho}_{n\mathbf{m}} - \boldsymbol{\rho}_{\mathbf{m}}$ (displacement of the vortices from their equilibrium positions, $\boldsymbol{\rho}_m$, in a perfect lattice):

$$\varphi_{n,n+1}(\boldsymbol{\rho}) = \frac{B}{s\Phi_0}\sum_{\mathbf{k},q} e^{-iqn}(1 - e^{iq})\boldsymbol{\mathcal{D}}(\boldsymbol{\rho},\mathbf{k})\mathbf{u}(q,\mathbf{k}). \tag{2.9}$$

The Fourier components of the distortions $\mathbf{u}_{n\mathbf{m}}$ are

$$\mathbf{u}(q,\mathbf{k}) = \frac{s\Phi_0}{B}\sum_{n,\mathbf{m}} u_{n\mathbf{m}}\exp(i\mathbf{k}\cdot\boldsymbol{\rho}_{\mathbf{m}} + iqn), \tag{2.10}$$

and, for a square vortex lattice, $\boldsymbol{\mathcal{D}}$ is given by

$$\boldsymbol{\mathcal{D}}(\boldsymbol{\rho},\mathbf{k}) = \frac{2\pi iB}{\Phi_0}\sum_{\mathbf{G}}\left[\frac{(k_y + G_y)\hat{\mathbf{x}} - (k_x + G_x)\hat{\mathbf{y}}}{|\,\mathbf{k} + \mathbf{G}\,|^2 + 2\lambda_J^{-2}(1 - \cos q) + \lambda_c^{-2}}\right]\exp[i(\mathbf{k} + \mathbf{G})\cdot\boldsymbol{\rho}]. \tag{2.11}$$

In Eq. (2.11), the summation is over the reciprocal lattice vectors $\mathbf{G}$. The linear approximation used gives a lower limit for $\varphi_{n,n+1}$ because it overestimates the effect of screening: $\sin\varphi_{n,n+1} < \varphi_{n,n+1}$. Notice that in the continuous limit (all $\mathbf{G} = 0$) the phase difference depends only on the transverse component of the distortion field.

Once the gauge-invariant phase difference $\varphi_{n,n+1}$ has been related to the vortex positions, the critical current between layers n and $n + 1$ can be obtained from

$$I_{n,n+1} = j_0\left|\int d\boldsymbol{\rho}\langle\exp[i\varphi_{n,n+1}(\boldsymbol{\rho})]\rangle\right|. \tag{2.12}$$

Here $\langle\cdots\rangle$ denotes either thermal averaging,

$$\langle A\rangle = \frac{\int D\mathbf{u}_{n,\mathbf{m}}A\{\mathbf{u}_{n,\mathbf{m}}\}\exp(-\beta\mathcal{F}\{\mathbf{u}_{n\mathbf{m}}\})}{\int D\mathbf{u}_{n\mathbf{m}}\exp(-\beta\mathcal{F}\{\mathbf{u}_{n\mathbf{m}}\})}, \tag{2.13}$$

where $\mathcal{F}\{\mathbf{u}_{n\mathbf{m}}\}$ is the free-energy functional of the distorted lattice, or impurity averaging, or both depending on the temperature regime and the presence or absence of pinning centers. Well above the irreversibility line, the main effect is the thermally induced disorder, whereas at low temperature, pinning-induced disorder represents the main effect. These two situations will now be examined carefully.

III. THERMALLY INDUCED DISORDER

A. Stack of superconducting layers

In the absence of pinning, i.e., above the irreversibility line, the phase difference from one layer to the next is generated by the thermal motion of the pancake vortices, and the determination of the critical current requires the evaluation in Eq. (2.12) of the thermal average Eq. (2.13). For simplicity, we describe the lattice distortions in the harmonic approximation and use for the free energy of the distorted lattice the following expression:

$$\mathcal{F}\{\mathbf{u}_{n\mathbf{m}}\} = \frac{B}{2s\Phi_0}\sum_{q,\mathbf{k}}\sum_{i,j}(c_{11}k^2\mathcal{P}_{L,ij} + c_{66}k^2\mathcal{P}_{T,ij} + \delta_{ij}c_{44}Q^2)u_i(q,\mathbf{k})u_j^*(q,\mathbf{k}), \tag{3.1}$$

where $\mathbf{k} = (k_x, k_y)$, $Q^2 = 2(1-\cos q)/s^2$, and $i, j = x, y$. $\mathcal{P}_{L,ij} = k_i k_j/k^2$ and $\mathcal{P}_{T,ij} = \delta_{ij} - \mathcal{P}_{L,ij}$ are longitudinal and transverse projection operators. c_{66}, c_{11}, and c_{44} are the flux lattice shear, compression, and tilt moduli, respectively. They are given by[11,19]

$$c_{44} = \frac{B^2}{4\pi(1+\lambda_c^2k^2+\lambda_{ab}^2Q^2)} + \frac{B\Phi_0}{32\pi^2\lambda_c^2}\ln\frac{\xi_{ab}^{-2}}{K_0^2+\lambda_J^{-2}} + \frac{B\Phi_0}{32\pi^2\lambda_{ab}^4Q^2}\ln\left(1+\frac{Q^2}{K_0^2}\right), \tag{3.2}$$

$$c_{11} = \frac{B^2[1+\lambda_c^2(k^2+Q^2)]}{4\pi[1+\lambda_{ab}^2(k^2+Q^2)](1+\lambda_c^2k^2+\lambda_{ab}^2Q^2)}, \quad c_{66} = \frac{B\Phi_0}{(8\pi\lambda_{ab})^2}.$$

The summation over $\mathbf{k}$ is performed over a circular Brillouin zone of radius $K_0^2 = 4\pi B/\Phi_0$.

In the Lawrence-Doniach formalism, λ_c and j_c are inter-related via Eq. (2.3):

$$\lambda_c^2(B) = \frac{c\Phi_0}{8\pi^2 s j_c(B)}, \; j_c(B) = \frac{I_{n,n+1}(B)}{\int d\boldsymbol{\rho}}, \tag{3.3}$$

where $I_{n,n+1}(B)$ is given by Eq. (2.12). In addition, $j_c(B)$ depends on $\lambda_c(B)$ via Eqs. (2.12)–(3.2). Thus Eqs. (2.12)-(3.3) allow one to obtain j_c, and hence the effective anisotropy parameter, $\gamma(B) = \lambda_c(B)/\lambda_{ab}$, self-consistently. This relationship between the (thermally averaged) critical current, the London penetration depth λ_c, and the tilt and compression moduli in the presence of a magnetic field is specific to the LD model and is responsible for the existence of the decoupling phase transition to be discussed below.

The integrand in Eq. (2.12) is now quadratic in the Fourier components of the distortion field and the resulting Gaussian integral can be done exactly. The final result is

$$I_{n,n+1} = j_0\int d\boldsymbol{\rho}\exp[-S(\boldsymbol{\rho})], \tag{3.4}$$

where

$$S(\boldsymbol{\rho}) = \frac{TB}{s\Phi_0}\sum_{\mathbf{k},q}\frac{1-\cos q}{k^2}\left[\frac{|\,\mathcal{D}_xk_y - \mathcal{D}_yk_x\,|^2}{c_{66}k^2+c_{44}Q^2} + \frac{|\,\mathcal{D}_xk_x + \mathcal{D}_yk_y\,|^2}{c_{11}k^2+c_{44}Q^2}\right]. \tag{3.5}$$

The coordinate dependent function $S(\boldsymbol{\rho})$ can be written as $S(\boldsymbol{\rho}) = S_0 + S_1(\boldsymbol{\rho})$, where S_0 is coordinate-independent. S_0 is obtained by keeping only the terms for which $\mathbf{G} = \mathbf{G}'$ in the double summation over $\mathbf{G}$ and $\mathbf{G}'$ in Eq. (3.5). S_0 represents the main contribution to the total sum in Eq. (3.5), and S_1 will be neglected henceforth. We get

$$S_0(\gamma) = \frac{TB}{s\Phi_0}\left(\frac{2\pi B}{\Phi_0}\right)^2\sum_{\mathbf{k},q}\sum_{\mathbf{G}}\frac{(1-\cos q)}{k^2[|\,\mathbf{k}+\mathbf{G}\,|^2 + 2\lambda_J^{-2}(1-\cos q)+\lambda_c^{-2}]^2}\left[\frac{[\mathbf{k}\cdot(\mathbf{k}+\mathbf{G})]^2}{c_{66}k^2+c_{44}Q^2} + \frac{[\hat{\mathbf{z}}\cdot(\mathbf{k}\times\mathbf{G})]^2}{c_{11}k^2+c_{44}Q^2}\right]. \tag{3.6}$$

The upper limit in the summation over $\mathbf{G}$ is $1/u_T$, where $u_T^2 \equiv \langle(\mathbf{u}_{n+1,\mathbf{m}} - \mathbf{u}_{n,\mathbf{m}})^2\rangle$ because the expansion of $\varphi_{n,n+1}$ in $u_{n,\mathbf{m}}$, Eq. (2.9), is valid only for wave vectors smaller than $1/u_T$.

The self-consistency equation for the effective anistropy parameter, $\gamma(B)$ is

$$\gamma^2 = \gamma_0^2\exp[S_0(\gamma)], \tag{3.7}$$

where γ_0 is the bare anisotropy parameter in the absence of magnetic field. The thermally averaged critical current density is $j_c(B) = j_0\gamma_0^2/\gamma^2(B)$. The transcendental equation for γ, Eq. (3.7), has to be solved numerically if all three terms appearing in the expression for c_{44}, Eq. (3.2), are kept. However, in some limiting cases, it is possible to proceed further analytically, namely, in the case of moderate anisotropies ($\gamma_0 \ll \lambda_{ab}/s$) or in the case of very large anisotropies ($\gamma_0 \gg \lambda_{ab}/s$).

For large anisotropies, only the third term in c_{44} plays a significant role. It represents the contribution to the tilt modulus arising from the electromagnetic coupling between the pancake vortices in adjacent layers. In addition, if we set $c_{66} = 0$, then the integration over q can

be performed exactly in Eq. (3.5). (The numerical computations show that c_{66} does not play a significant role in determining the value of the critical current, so this is a reasonable approximation.) In the large magnetic field limit, $B \gg B_{cr} \equiv 2\Phi_0/4\pi\gamma_0^2 s^2$, the final result is

$$S_0(\gamma) = \frac{2\pi^2 BT\lambda_{ab}^2(T)}{s\Phi_0^3} \frac{\ln(K_0^2\gamma^2 s^2/2)}{\ln(2s^{-2}K_0^{-2})}. \tag{3.8}$$

Notice that we kept the $\mathbf{G} = 0$ term only in the summation over $\mathbf{G}$; additional terms do not contribute significantly and will be accounted for in the numerical calculation to be discussed below. The self-consistency equation, Eq. (3.7), becomes

$$\frac{\gamma^2}{\gamma_0^2} = \left(\beta\frac{\gamma^2}{\gamma_0^2}\right)^{\alpha}, \tag{3.9}$$

where

$$\alpha = \frac{2\pi^2 BT\lambda_{ab}^4(T)}{s\Phi_0^3 \ln(2s^{-2}K_0^{-2})}, \quad \beta = \frac{K_0^2 s^2\gamma_0^2}{2} = \frac{B}{B_{cr}}. \tag{3.10}$$

The solution of this equation is

$$\gamma^2 = \gamma_0^2\beta^{\alpha/(1-\alpha)}, \tag{3.11}$$

for $\alpha < 1$ ($\beta \gg 1$) and $\gamma = \infty$ for $\alpha > 1$. Notice that γ increases continuously with α so that we have a second-order phase transition along the line $\alpha(T, B) = 1$ in the H-T plane. The magnetic field along this line is the decoupling field:

$$B_D(T) = \frac{\Phi_0^3 s}{32\pi^3 T\lambda_{ab}^4(T)} \ln\left(\frac{8\pi^2 T\lambda_{ab}^4}{\Phi_0^2 s^3}\right). \tag{3.12}$$

This phase transition is very smooth: the temperature derivatives of γ (or equivalently, j_c) at the phase transition are continuous. In particular, there is no specific heat anomaly at the phase transition (as for a Kosterlitz-Thouless phase transition for instance).

From a physical point of view, at $B_D(T)$ the root-mean-square thermal distortion $u_T = \langle(u_{n+1,\mathbf{m}} - u_{n,\mathbf{m}})^2\rangle^{1/2}$ becomes comparable to the intervortex distance [$\simeq (\Phi_0/B)^{1/2}$]. The pancake vortices in a given flux line are not correlated for $B > B_D(T)$, and in that sense the flux *lines* do not exist; the motion of the pancake vortices in adjacent layers is uncorrelated, the phase difference is completely random, and the critical current along the c axis vanishes.

For moderate anisotropies, the third term in c_{44}, Eq. (3.2), is unimportant, while the other two terms are of the same order of magnitude for $k \simeq K_0$. In order to understand at least qualitatively the nature of the phase transition at the decoupling field in this case, we keep only the first term in the expression for c_{44}. (The numerical calculations show that adding the second term does not change the results qualitatively.) In this limit, one can show that

$$S_0(\gamma) = \frac{\pi TBs\lambda_{ab}^2\gamma^2}{2\Phi_0^3}, \tag{3.13}$$

and the self-consistency equation reduces to

$$x = \exp(\delta x), \quad x = \gamma^2/\gamma_0^2, \tag{3.14}$$

where

$$\delta = \frac{\pi TBs\lambda_{ab}^2\gamma_0^2}{2\Phi_0^3}. \tag{3.15}$$

The solution to this equation exists for $\delta < 1/e$ (e is the natural logarithm basis). At $\delta = 1/e$, x increases suddenly from e to infinity, i.e., the critical current decreases continuously from j_0 at $B = 0$ to $j_0 e^{-1}$ at $B = B_D(T)$ and vanishes for $B > B_D(T)$. The decoupling field is now given by the condition $\delta = 1/e$, i.e.,

$$B_D(T) = \frac{2\Phi_0^3}{\pi eTs\lambda_{ab}^2(T)\gamma_0^2}. \tag{3.16}$$

The phase transition at the $B_D(T)$ line is now a first-order phase transition. The free energy density of the system can be calculated from the following expression:

$$\frac{\partial F}{\partial\gamma_0^{-2}} = -\frac{\Phi_0^2}{16\pi^3 s^2\lambda_{ab}^2}\langle\cos\varphi_{n,n+1}\rangle = -\frac{\Phi_0^2}{16\pi^3 s^2\lambda_{ab}^2}\exp[-S_0(\gamma)], \tag{3.17}$$

and S_0 depends on γ_0 implicitly. After integrating over γ_0^{-2}, one obtains the following expression for the free-energy density:

$$F(\gamma_0) = F(\infty) - \frac{\Phi_0^2}{32\pi^3 s^2\lambda_{ab}^2}\left[\left(\frac{1}{\gamma^2} - \frac{e}{\gamma_0^2}\right) - \ln\frac{\gamma_0^2}{\gamma^2}\right], \tag{3.18}$$

where γ is now a function of γ_0 through the self-consistency condition for γ, Eq. (3.14). The latent heat (per unit volume) can be calculated from the expression for the free energy:

$$\Delta Q = \frac{\Phi_0^2}{32e\pi^3\lambda_{ab}^2(T)s^2\gamma_0^2}. \tag{3.19}$$

So, for large anisotropies, the phase transition at the decoupling field is second order, whereas for small anisotropies it is first order. There is a smooth transition from first to second order at some critical value of γ_0. For the parameters used in Figs. 2 and 3, this value is $\gamma_0 \simeq 60$. This value seems to be temperature independent.

The dependence of the critical current on magnetic field and temperature obtained from a numerical resolution of the self consistency equation is shown in Figs. 2 and 3 for two different values of γ_0. The decoupling field is shown in Fig. 4 for $\gamma_0 = 30$ and 55. The experimental data for $Bi_2Sr_2CaCu_2O_8$ is taken from Ref. 20. The decoupling curve taken from Ref. 20 as well as the calculated decoupling lines lie above the irreversibility line for $Bi_2Sr_2CaCu_2O_8$.[2]

We used the harmonic approximation for the elastic energy to study quantitatively the decoupling transition. Actually, the anharmonic effects that are important for melting transition may affect the decoupling transition as well. They enhance the vortex distortions and thus may decrease the transition temperature $T_D(H)$. We have

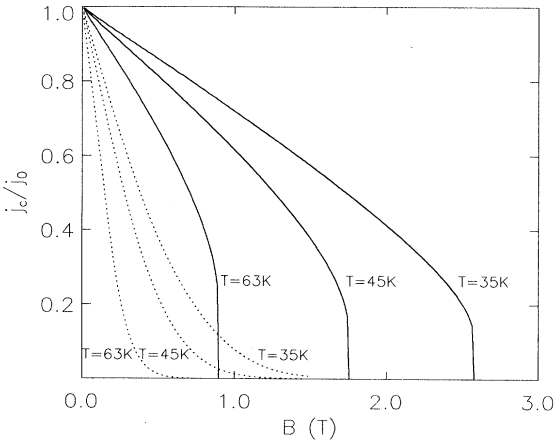

FIG. 2. Magnetic field dependence of the critical current along the c axis in a single crystal. The solid lines correspond to $\gamma_0 = 55$; the dashed lines correspond to $\gamma_0 = 200$.

assumed a flux lattice in our calculations, but a flux liquid would lead to the same results because of the very weak dependence of j_c on c_{66}. (A numerical calculation with $c_{66} = 0$ showed that this was indeed the case.)

It is important to emphasize that the mechanism described above is only one mechanism among other physically possible dissipation mechanisms that can affect the critical current along the c axis in perpendicular fields. For example, the current flowing along the c axis generates a magnetic field (the so-called self-field) in addition to the applied magnetic field. In samples whose transverse dimensions are larger than λ_J, the self-field can generate Josephson vortices between the ab planes. These vortices form concentric "rings" that move inward, and in doing so they dissipate energy. This current limiting mechanism would presumably lead to a critical current smaller than the critical current calculated above. It is still true, however, that the phenomenological parameters γ (and thus λ_c) must be determined self-consistently,

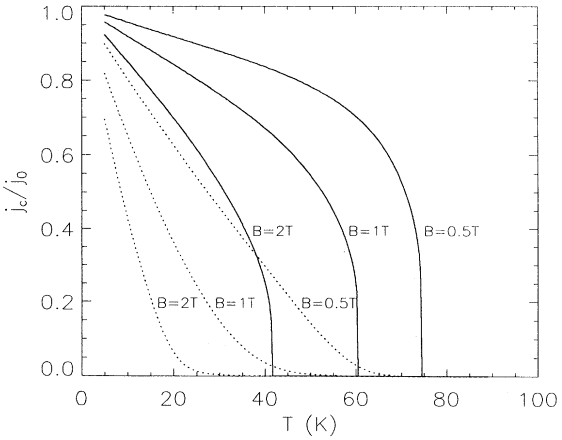

FIG. 3. Temperature dependence of the critical current along the c axis in a single crystal. The solid lines correspond to $\gamma_0 = 55$; the dashed lines correspond to $\gamma_0 = 200$.

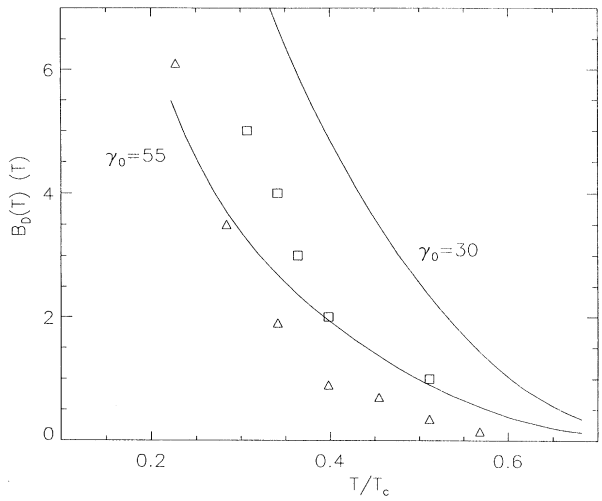

FIG. 4. Temperature dependence of the decoupling field for two values of γ_0 calculated for $s = 15$ Å, $\lambda_{ab}(0) = 1500$ Å, and $\xi_{ab}(0) = 25$ Å. The triangles denote data obtained from transport critical current measurements with a voltage criterion of 3μV. The squares were obtained by fitting the I-V curves to a phenomenological equation. See Ref. 20 for details.

regardless of the physical mechanism limiting the critical current. In samples whose dimensions are such that $R_c < \gamma s = \lambda_J$, the formation of Josephson vortices is supressed and the critical current coincides with the critical current calculated above.

Finally, it is interesting to consider how the recent c-axis resistivity measurements of Refs. 2 and 3 could be accounted for by the mechanism just described. Below T_c, the resistivity $\rho_c(T)$ increases exponentially with decreasing temperature:

$$\rho_c(T) = AT^{\nu} \exp(-\Delta/T), \tag{3.20}$$

where $\nu \approx 0.7$ and $\Delta \approx 176$ K. This simple empirical relation was proposed in Refs. 21 and 22 and seems to describe the experimental data quite well. The exponential dependence of ρ_c on temperature was attributed to quasiparticle tunneling and Δ was associated with the superconducting energy gap. According to these experimental observations the layers are still *superconducting* well below T_c (the gap in the quasiparticle spectrum is nonzero) but the interlayer supercurrent vanishes. Below a certain temperature, Eq. (3.20) ceases to be valid, and the resistivity starts decreasing until it vanishes at some temperature $T_0(H)$, which is well below the temperature corresponding to the maximum in the resistivity curve [where Eq. (3.20) no longer applies]. We identify the temperature T_0 with the decoupling temperature $T_D(H)$. In a mean-field approach for the decoupling phase transition, one would expect the resistivity to drop suddenly to zero at a temperature $T_D(H)$ below, which the Josephson supercurrent becomes nonzero. Beyond the mean-field approach, above $T_D(H)$, fluctuations of the Josephson current are important, they contribute to the conductivity, smear out the sharp mean-field transition, and lead

to a temperature dependence of the resistivity similar to that observed experimentally.

B. Josephson junction parallel to the c axis

Consider a weak link formed by two adjacent superconducting grains such that the plane of the junction contains the c axis and the a or b axis [Fig. 1(b)]. The external magnetic field is still applied along the c-axis. It nucleates vortices on each side of the junction. The ab-plane critical current for this ab weak link is again affected by the presence of vortices on each side of the plane of the junction. If the vortices form a regular hexagonal lattice, the phase difference is determined by the standard expression $z_f(H)Hy/\Phi_0$, which leads to the usual Fraunhofer dependence of the critical current on H. Here $z_f(H)$ is the effective thickness of the junction introduced in Ref. 7. However, if the vortices are disturbed from their equilibrium position, e.g., because of thermal vibrations at finite temperature, an additional random-phase difference is generated across the junction and the critical current is depressed locally. The mechanism is similar to that described above, but the phase difference is now due to the "mismatch" of two pancake vortices belonging to two different flux lines rather than being associated with the misalignement of two pancake vortices located in adjacent layers but belonging to the same flux line. This particular situation has been considered previously by Fistul'[23] and Denisov.[24] Fistul', however, considered the effect of randomly distributed vortices without identifying the source of disorder. Thermally induced disorder and (weak) pinning-induced disorder have well-defined properties that are not reflected in Fistul's assumptions and calculations.

As a first approximation, we can still use Eq. (2.8) as a solution to the Laplace equation for the phase difference, but we have to modify this solution slightly to take into account explicitly the presence of the junction boundary. This can be done easily by using images. The solution for the phase difference is then

$$\varphi_{12}(y) = 2\sum_{\mathbf{m}}\left(\arctan\frac{x_{1\mathbf{m}}}{y-y_{1\mathbf{m}}} - \arctan\frac{x_{2\mathbf{m}}}{y-y_{2\mathbf{m}}}\right) + \frac{z_f H y}{\Phi_0}, \tag{3.21}$$

where the subscript $\mathbf{m}$ is used to label the vortices and the subscripts 1 and 2 refer to vortices in the left- and right-hand side of the junction, respectively. In the summation over $\mathbf{m}$ in Eq. (3.21) the vortices at distances smaller than λ_J and λ_{ab} from the junction only should be taken into account. For distances larger than λ_J the phase difference due to vortices is reduced by the Josephson interlayer currents, whereas at distances larger than λ_{ab} the electromagnetic screening becomes important and decreases the phase difference induced by the vortices.[24] The rest of the calculation of the critical current is similar to that detailed in the preceding section for a stack of superconducting layers. There are, however, some differences: the factor $(1-\cos q)$ in Eq. (3.6) should be omitted and the elastic moduli should be altered to take into account the presence of the boundary. This latter step can be accomplished approximately by replacing B by $2B$ in the expressions for the moduli. This accounts for the fact that there are now twice as many vortices within a distance λ_{ab} from the boundary (the vortices plus their images). Another important difference is that self-consistency is not required here, and therefore there is no decoupling phase transition for the junction under consideration. Otherwise, the results are qualitatively similar to those obtained for a stack of superconducting layer in perpendicular magnetic field. The ab weak links could play an important role in limiting the critical current in superconducting tapes, and a more detailed discussion will be given elsewhere.

IV. PINNING-INDUCED DISORDER

Let us now consider the effect of pinning centers on the critical current along the c axis. It has been known for a long time that even weak pinning centers causes the long-range order in the arrangement of the flux lines to be lost. In addition, because of the random distribution of the pinning centers in the direction perpendicular to the layers, the flux lines can bend significantly, causing further distortions in the 3D arrangement of pancake vortices. Notice that in what follows we do not consider "correlated disorder," such as columnar defects, or other macroscopic microstructural defects, such as twinning planes. We consider the effect of randomly distributed point defects only.

In the case of weak disorder, the flux lattice is elastically distorted and the distortions can be calculated in the harmonic approximation. The important point to notice is that the displacements in this approximation are all longitudinal in the continuum limit [all $\mathbf{G}$ set equal to zero in Eq. (3.5)]. In this limit, the gauge-invariant phase difference *vanishes*. So, the effect of weak disorder from weak pinning center is *nil* (in the continuum approximation). The critical current along the c axis is not affected significantly. This is in contrast to the effect of thermal disorder: the two situations are qualitatively very different even though the order of magnitude of the distortions, $\langle u_{n\mathbf{m}}\rangle$, is comparable in both cases. This is due to the absence of small wave-vector contributions in the case of pinning-induced disorder. Those represent the main effect in the case of thermal disorder.

In order for pinning to have a significant effect on the critical current along the c axis, we have to go beyond the elastically distorted lattice, i.e., we have to consider the effect of *plastic* deformations of the flux lattice. Such deformations can be induced by very strong pinning centers, and we now estimate crudely their effect on the critical current.

First, let us consider small magnetic fields. In this case, the lattice is relatively "soft" and a few strong pinning centers are presumably enough to distort the lattice plastically. Our main assumption is the following: consider two pancake vortices in layers n and $n+1$ belonging to the same flux line. The pancake vortex in layer $n+1$ is shifted towards the nearest pining center if the pinning energy ϵ_p is larger than the energy ϵ_d needed to create

the corresponding distortion in the flux lattice. The pinning energy, ϵ_p is given by the ususal expression for core pinning:

$$\epsilon_p = \frac{C_1 \Phi_0^2 s}{16\pi^2 \lambda_{ab}^2}, \tag{4.1}$$

where C_1 is a numerical constant of order unity. The order of magnitude of the energy needed to create a dislocation by shifting a pancake vortex a distance $u \gtrsim \lambda_J$ from its equilibrium position is[15]

$$\epsilon_d \simeq \frac{\Phi_0^2 u}{4\pi^2 \lambda_{ab} \lambda_c}. \tag{4.2}$$

This corresponds to the energy it takes to shift a single pancake vortex a distance u for moderate anisotropy. Therefore, a vortex will be shifted if there is a strong pinning center a distance $u < u_0 \simeq \lambda_J$ from its equilibrium position, otherwise it remains at its equilibrium location. The gauge-invariant phase difference is now given by

$$\varphi_{n,n+1}(\rho) = \sum_{\mathbf{m}} \mathcal{D}(\boldsymbol{\rho} - \boldsymbol{\rho}_{\mathbf{m}}) \cdot \mathbf{u}_{\mathbf{m}}, \tag{4.3}$$

where

$$\mathcal{D}(\boldsymbol{\rho}) = \left(\frac{y}{\rho^2}, -\frac{x}{\rho^2} \right), \tag{4.4}$$

and after subtitution in Eq. (3.5), we should average over the positions of the pinning centers:

$$I_{n,n+1} = j_0 \left| \int d\boldsymbol{\rho} \prod_{\mathbf{m}} \left\{ 1 + \int_{u<u_0} d\mathbf{u} \ \{ \exp[i\mathcal{D}(\boldsymbol{\rho} - \boldsymbol{\rho}_{\mathbf{m}}) \cdot \mathbf{u}_{\mathbf{m}}] - 1 \} \, p(\mathbf{u}_{\mathbf{m}}) \right\} \right|. \tag{4.5}$$

The probability density $p(\mathbf{u}_{\mathbf{m}}) = n/\pi$, where n is the areal density of pinning centers and corresponds to a uniform distribution of pinning centers in the ab-planes. Notice that in Eq. (4.5), we treat the vortices as independent, i.e., we consider the weak magnetic field limit: $B \ll \Phi_0/4\pi\lambda_J^2, \Phi_0 n$.

If the pinning center density is low ($\lambda_J \ll n^{-1/2}$), a pancake vortex in layer $n+1$ cannot always find a pinning center nearby. In this limit, one can show that Eq. (4.5) simplifies to

$$I_{n,n+1} = j_0 \left| \int d\boldsymbol{\rho} \exp\left\{ -\sum_{\mathbf{m}} \pi^{-1} n u_0^2 \times \left[1 - 2\frac{J_1(u_0 \mid \boldsymbol{\rho} - \boldsymbol{\rho}_{\mathbf{m}} \mid^{-1})}{u_0 \mid \boldsymbol{\rho} - \boldsymbol{\rho}_{\mathbf{m}} \mid^{-1}} \right] \right\} \right|. \tag{4.6}$$

$J_1(x)$ is the Bessel function of the first kind of order one. Upon replacing the summation over $\mathbf{m}$ by an integral and evaluating the resulting expression, we obtain

$$j_c(B) \simeq j_0 \exp\left(-\frac{\pi n^2 u_0^6 B}{8\Phi_0} \right). \tag{4.7}$$

In the opposite limit, $\lambda_J \gg n^{-1/2}$, there are enough pinning centers that each pancake vortex can easily find one in its vicinity, and we can assume that all the pancake vortices are shifted from their equilibrium positions. A simple calculation similar to the one performed above for the low density of pining centers case shows that

$$j_c(B) \simeq j_0 \exp\left(-\frac{\pi B}{2n\Phi_0} \right). \tag{4.8}$$

In this case, the critical current *increases* with increasing n. So, the critical current decreases at first as the concentration of pinning centers is increased, but then increases back to its maximum value j_0 as the concentration of pinning centers continues to increase. This is not very surprising because in the limit of small B and large n, each pancake vortex can find a pinning center very close to its equilibrium position in the undistorted flux lattice, and hence the flux lattice as a whole remains undistorted, or at least very weakly distorted. The initial decrease at low magnetic fields of the critical current in irradiated samples was observed recently by Gerhäuser *et al.*[25] The effect of disorder in "*ab*" weak links is similar to that described above.

The effect of strong disorder in the large magnetic field limit remains to be studied. In principle, at high magnetic fields, the decoupling transition is possible at large concentrations of strong pinning centers, as in the case of thermal disorder.

V. APPLICATION TO TAPES AND FILMS

The "vortex fluctuation" mechanism described above should apply to tapes and films as well. Their microstructure is such that a description in terms of Josephson-coupled subsystems should be adequate. Numerous microstructural studies have revealed that tapes and in some cases films, of the high-T_c materials are made of a superposition and juxtaposition of *c*-axis oriented grains. The orientation of the $\hat{a}$ and $\hat{b}$ axes of a grain is random in the plane of the tape (or film). We can assume that the *c*-axis grain boundaries (in the plane of the tape) are fairly well coupled and form weak links across which a significant amount of current can flow, whereas the grain boundaries between two adjacent twisted grains are such that no significant current can flow across them. This assumption leads Malozemoff to introduce the "brick-wall" model.[6] In this simplified description of the tape microstructure, the grains are modeled by "bricks" arranged at random (Fig. 5). The current flows along the tape axis, but can flow in a given grain only as long as it does not encounter a grain boundary between two adjacent brick. At this point, it chooses the path of least resistance, namely, it transfers along a *c*-axis grain boundary to the grain below or above. If pinning at intergrain boundaries is large enough to sustain a significant current within a grain, the bottleneck for current flow along a tape is the weak links associated with the *c*-axis grain boundaries. In other words, it is assumed that the in-

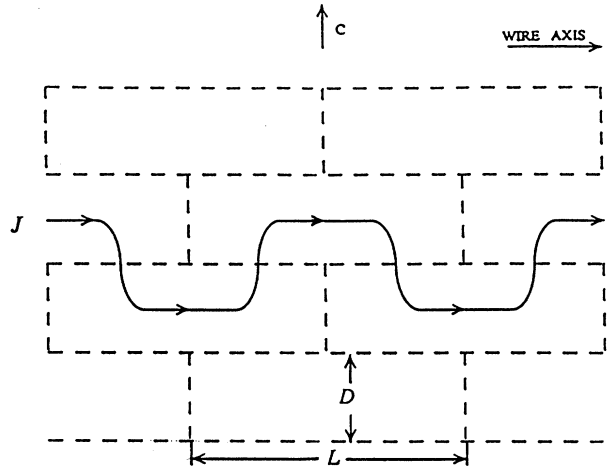

FIG. 5. Schematic representation of the brick-wall model microstructure.

tergrain critical current along the c-axis rather than the ab-plane critical current that limits the current flow along the tape axis.

The critical current associated with a weak link is affected by the presence of a magnetic field. When the magnetic field is applied parallel to the tape axis, the critical current was calculated by Bulaevskii *et al.*[7] If the magnetic field is parallel to the c axis, however, vortices are nucleated inside the grains and the above described vortex fluctuation mechanism applies for intergrain critical current.

At low temperatures, we can neglect the effect of thermal distortions and consider the effect of pinning only. The strongest pinning mechanism is provided by the intergrain a- and b-axis tilt boundaries (oriented perpendicular to the ab planes). The electron density and, correspondingly, the superconducting order parameter are supressed at such a boundary because the tilting of the CuO_2 planes destroys the covalent bonds there. Vortices are strongly trapped by these a- and b-axis tilt boundaries. These boundaries determine the position of the vortex lattice inside the grains. At c-axis twist boundaries (parallel to the ab planes) the vortex lines jump from one arrangement in the top grain to another in the bottom grain (forming a piece of Josephson vortex inside the boundary). The shift of pancakes along the vortex line at a c-axis boundary $\mathbf{u}$ is random. In strong magnetic fields $B \gg H_{c1,\perp}$ we have $u \lesssim l$, where $l = \sqrt{\Phi_0/B}$ is the intervortex distance. We assume that the statistical distribution of $\mathbf{u}$ is a Gaussian with standard deviation of the order of the intervortex distance:

$$p(\mathbf{u}) = \frac{bB}{\pi\Phi_0} \exp\left(-\frac{bBu^2}{\Phi_0}\right), \tag{5.1}$$

where b is of order unity. We consider fields $B \gg n\Phi_0$, where n is the concentration of pinning centers in a layer (if $B \ll n\Phi_0$ the dispersion does not depend on B). The final result for the intergrain critical current is

$$\frac{j_c(B)}{j_c(0)} = \frac{\int d\boldsymbol{\rho} \int d\mathbf{u} p(\mathbf{u}) \exp(i \sum_{\mathbf{m}} \mathcal{D}(\boldsymbol{\rho} - \boldsymbol{\rho}_{\mathbf{m}}) \cdot \mathbf{u})}{\int d\boldsymbol{\rho}}. \tag{5.2}$$

The upper limit for the summation over $\mathbf{m}$ is determined by L if $L < \overline{\lambda_J}$ and by $\overline{\lambda_J}$ if $\overline{\lambda_J} < L$ ($\mid \boldsymbol{\rho} - \boldsymbol{\rho}_{\mathbf{m}} \mid < L$), where L is a typical grain length and $\overline{\lambda}_J$ is the Josephson length of the c-axis boundary Josephson junction:

$$\overline{\lambda}_J = c\Phi_0/16\pi^2 j_c(B)\Lambda, \tag{5.3}$$

where Λ=min(λ_{ab}, D) and $\overline{\lambda}_J \leq \lambda_J$. After performing the summation over $\mathbf{m}$, we obtain the following expression for the critical current:

$$j_c(B)/j_c(0) = (B_0/B)^{\nu}, \tag{5.4}$$

where $\nu = \pi/4b$ and $B_0 = \max(\Phi_0/L^2, \Phi_0/\overline{\lambda_J}^2)$. For tapes and not very perfect films we can assume that $L < \overline{\lambda}_J$, and Eq. (5.4) provides the final result with $B_0 = \Phi_0/L^2$. The perfect films seems to behave more like single crystal. For them we can assume that $\overline{\lambda}_J$ is close to λ_J and $\overline{\lambda}_J < L$. Then $j_c(B)$ should be determined self-consistently because $\overline{\lambda}_J$ depends on $j_c(B)$, see Eq. (5.3). The final result for perfect films is:

$$\frac{j_c(B)}{j_c(0)} = \left[\frac{8\pi^2\lambda_{ab}^2 D j_c(0)}{cBsL}\right]^{\nu/(1-\nu)}. \tag{5.5}$$

Experimental data for films and tapes is shown in Fig. 6 for a $Bi_2Sr_2Ca_2Cu_3O_{10}$ tape at 20 K (Ref. 4) and for a $Bi_2Sr_2CaCu_2O_8$ films at various temperatures.[26,27] The data for tape is well described by Eq. (5.4) with $\alpha \simeq 0.3$, i.e., $b \simeq 2 - 2.5$. For films, Eq. (5.5) fits the data with approximately the same ν. For low fields, $B \ll n\Phi_0$, the results (4.7) and (4.8) can be used but now u_0 is determined by including also the electromagnetic contribution in ϵ_d, which becomes important in the case of large λ_J.[15] Hence, in the low-field limit, the field dependence of the critical current is approximatly linear and a crossover from Eq. (5.4) to a linear dependence occurs at $B \simeq \Phi_0 n$.

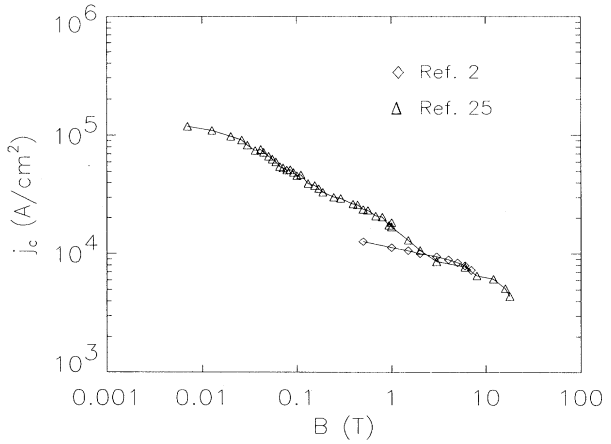

FIG. 6. Low temperature magnetic field dependence of the critical current in a $Bi_2Sr_2Ca_2Cu_3O_{10}$ tape (Ref. 4) and a $Bi_2Sr_2CaCu_2O_8$ film (Ref. 26) for $H \parallel \hat{c}$.

Thermal disorder affects the critical current along the c axis via the same mechanism at work in single crystals. The main difference is that in tapes the weaker intergrain Josephson coupling rather than the interlayer Josephson coupling limits the critical current. Also, the grains have a finite length in the ab plane. The coupling between the vortices across a c-axis grain boundary is mostly electromagnetic in origin, and therefore we use the same expression as in single crystal for $S_0(\gamma)$ but in the expression for c_{44}, Eq. (3.2), we neglect the first two terms and replace λ_J by L in the lower cutoff for the summation over $\mathbf{k}$. The order of magnitude of the critical current in this approximation is

$$\frac{j_T}{j_0} = \exp\left\{-\frac{32\pi^3 BT\lambda_{ab}^4(T)}{s\Phi_0^3}\frac{\ln[L/\lambda_{ab}(T)]}{\ln[1/(K_0 s)]}\right\}, \quad B \gg \frac{\Phi_0}{\lambda_{ab}^2}. \tag{5.6}$$

This is clearly a lower limit for the critical current, since we have assumed electromagnetic coupling between all the layers, whereas inside the bricks, the layers are in fact Josephson coupled. Because of the finite size of the system, there should be no decoupling phase transition.

VI. CONCLUSION

We have identified the physical mechanism, whereby in a Josephson-coupled system in perpendicular magnetic field, the critical current along the c axis is reduced due to pancake vortices misalignements. We examined the effect of thermally induced distortions as well as distortions caused by pinning centers. We showed that their effect on the critical current is qualitatively different. More importantly, we emphasized that within the framework of the LD model, the anisotropy parameter γ is renormalized by the thermally induced vortex fluctuations and has to be calculated in a self-consistent manner in the presence of a perpendicular field. This leads to the decoupling phase transition, the nature of which was elucidated. Application to tapes and films was considered within the framework of the brick-wall model and resonable agreement with experimental data was obtained.

It should be emphasized that the brick-wall model has received limited experimental verification so far. However, our conclusions regarding the critical current along the c axis for tapes in perpendicular fields are independent of whether the brick-wall model is an accurate description of the tapes or not. Our predictions for tapes could be checked by direct measurements of the critical current along the c axis. If the transfer of current along the c axis is indeed the limiting factor, the critical currents measured along the tape axis or perpendicular to it should be the same up to a geometrical aspect ratio: $j_c/j_{ab} = D/L$, and their temperature and field dependences should be similar. This in turn would provide additional support for the brick-wall model. Our results, Eqs. (5.4) and (5.6) are also applicable to single Josephson junctions made of highly anisotropic superconductors such as Bi- and Tl-based high-T_c compounds.

ACKNOWLEDGMENTS

This work was supported by the U.S. Department of Energy. We thank L.I. Glazman, B.I. Ivlev, V.G. Kogan, and M. Ledvij for useful discussions.

[1] W.E. Lawrence, S. Doniach, in *Proceedings of the 12th International Conference on Low Temperature Physics, Kyoto, 1970,* edited by E. Kanda (Keigaku, Tokyo, 1970).
[2] A. Kapitulnik, in *Phenomenology and Applications of High Temperature Superconductors*, edited by K. Bedell *et al.* (Addison-Wesley, Reading, MA, 1992), p. 34.
[3] G. Briceño, M.F. Crommie, and A. Zettl, Phys. Rev. Lett. **66**, 2164 (1991).
[4] M.P. Maley, P.J. Kung, J.Y. Coulter, W.L. Carter, G.N. Riley, and M.E. McHenry, Phys. Rev. B **45**, 7566 (1992).
[5] J.E. Tkaczyk, J.A. Deluca, P.L. Karas, P.J. Bednarczyk, M.F. Garbauskas, R.H. Arendt, K.W. Lay, and J.S. Moodera, Appl. Phys. Lett. **61**, 610 (1992); M.P. Maley, J. Appl. Phys. **70**, 6189 (1991).
[6] A.P. Malozemoff, in *Superconductivity and its Applications (Buffalo, 1991)* Proceedings of the Conference on Superconductivity and its Applications, AIP Conf. Proc. No. 251, edited by Y. H. Kao *et al.* (AIP, New York, 1992), p. 6.
[7] L.N. Bulaevskii, J.R. Clem, L.I. Glazman, and A.P. Malozemoff, Phys. Rev. B **45**, 2545 (1992).
[8] A. Buzdin and D. Feinberg, J. Phys. (Paris) **51**, 1971 (1990).
[9] J.R. Clem, Phys. Rev. B **43**, 7837 (1991).
[10] S.L. Miller, K.R. Biagi, J.R. Clem, and D.K. Finnemore, Phys. Rev. B **31**, 2684 (1985).
[11] L.I. Glazman and A.E. Koshelev, Phys. Rev. B **43**, 2835 (1991); Physica C **173**, 180 (1991).
[12] L.L. Daemen, L.N. Bulaevskii, M.P. Maley, and J.Y. Coulter, Phys. Rev. Lett. **70**, 1167 (1993).
[13] A. Barone, *Physics and Applications of the Josephson Effect* (Wiley, New York, 1984).
[14] L.N. Bulaevskii and J.R. Clem, Phys. Rev. B **44**, 10234 (1991); S.N. Artemenko and A.N. Kruglov, Physica C **173**, 125 (1991).
[15] L.N. Bulaevskii, M. Ledvij, and V. Kogan, Phys. Rev. B **46**, 366 (1992)
[16] A.A. Golubov, and M.Y. Kuprijanov, Zh. Eksp. Teor. Fiz. **92**, 1512 (1987) [Sov. Phys. JETP **65**, 849 (1987)].
[17] M.V. Fistul', Pis'ma Zh. Eksp. Teor. Fiz. **52**, 823 (1990) [Sov. JETP Lett. **52**, 192 (1990)].
[18] V.N. Gubankov, M.P. Lisitskii, I.L. Serpuchenko, and M.V. Fistul', Zh. Eksp. Teor. Fiz. **100**, 1326 (1991) [Sov. Phys. JETP **73**, 734 (1991)].
[19] E.H. Brandt, J. Low Temp. Phys. **26**, 709 (1977); **28**, 291 (1977).
[20] T. Fukami, T. Yamamoto, T. Nishizaki, Y. Horie, F. Ichikawa, T. Aomine, E. Holguin, and L. Rinderer, Solid State Commun. **70**, 605 (1992).
[21] M.F. Crommie and A. Zetll, Phys. Rev. B **43**, 408 (1991).
[22] D.H. Kim, K.E. Gray, R.T. Kampwirth, and D.M. McKay,

Phys. Rev. B **42**, 6249 (1990).
[23]M.V. Fistul', Zh. Eksp. Teor. Fiz. **96**, 369 (1989) [Sov. Phys. JETP **69**, 209 (1989)].
[24]Yu.P. Denisov, Zh. Eksp. Teor. Fiz. **45**, 90 (1963) [Sov. Phys. JETP **18**, 66 (1964)].
[25]W. Gerhauser, G. Ries, H.W. Neumüller, W. Schmidt, O. Eibl, G. Saemann-Ischenko and S. Klaumünzer (unpublished).
[26]S. Labdi, H. Raffy, O. Laborde, and P. Monceau, Physica C **197**, 274 (1992).
[27]P. Schmitt, L. Schultz, and G. Saemann-Ischenko, Physica C **168**, 475 (1990).